Entanglement distance for arbitrary M -qudit hybrid systems

(Article begins on next page)

28 January 2025

Entanglement distance for arbitrary M-qudit hybrid systems

Denise Cocchiarella, Stefano Scali, Salvatore Ribisi, Bianca Nardi, Ghofrane Bel-Hadj-Aissa, Roberto Franzosi

Entanglement distance for arbitrary M-qudit hybrid systems

Denise Cocchiarella,[1] Stefano Scali,[2, 3] Salvatore Ribisi,[4] Bianca
Nardi,[1] Ghofrane Bel-Hadj-Aissa,[1, 5] and Roberto Franzosi[5, *]

[1]*DSFTA, University of Siena, Via Roma 56, 53100 Siena, Italy*
[2]*Department of Physics, University of Cambridge, Cambridge CB3 0HE, United Kingdom*
[3]*Department of Physics and Astronomy, University of Exeter, Exeter EX4 4QL, United Kingdom*
[4]*Centre de Physique Théorique, Aix-Marseille University,*
Campus de Luminy, Case 907, 13288 Marseille Cedex 09, France
[5]*QSTAR & CNR - Istituto Nazionale di Ottica, Largo Enrico Fermi 2, I-50125 Firenze, Italy*

The achievement of quantum supremacy boosted the need for a robust medium of quantum information. In this task, higher-dimensional qudits show remarkable noise tolerance and enhanced security for quantum key distribution applications. However, to exploit the advantages of such states, we need a thorough characterisation of their entanglement. Here, we propose a measure of entanglement which can be computed either for pure and mixed states of a M-qudit hybrid system. The entanglement measure is based on a distance deriving from an adapted application of the Fubini-Study metric. This measure is invariant under local unitary transformations and has an explicit computable expression that we derive. In the specific case of M-qubit systems, the measure assumes the physical interpretation of an obstacle to the minimum distance between infinitesimally close states. Finally, we quantify the robustness of entanglement of a state through the eigenvalues analysis of the metric tensor associated with it.

I. INTRODUCTION

Entanglement is an essential resource for progressing in the field of quantum-based technologies. Quantum information has confirmed its importance in quantum cryptography and computation, in teleportation, in the frequency standard improvement problem and metrology based on quantum phase estimation [1]. The achievement of quantum supremacy [2] together with the rapid experimental progress on quantum control is driving the interest in entanglement theory. Nevertheless, despite its key role, entanglement remains elusive and the problem of its characterisation and quantification is still open [3, 4]. In time, several different approaches have been developed to quantify the variety of states available in the quantum regime [5]. Entropy of entanglement is uniquely accepted as measure of entanglement for pure states of bi-partite systems [6], while for the same class of mixed states, entanglement of formation [7], entanglement distillation [8–10] and relative entropy of entanglement [11] are largely acknowledged as faithful measures. The development of quantum information theory and the increasing experimental demand of quantum states manipulation led to develop measures enfolding more general states. For multi-partite systems a broad range of measures has covered pure states [12, 13] and mixed states [14] among which, a Schmidt measure [15] and a generalisation of concurrence [16] have been proposed. In the last years, the variety of paths adopted to tackle the problem led to estimation-oriented approaches based on the quantum Fisher information [17–19]. Due to the deep connection between the quantum Fisher informa-

tion and a statistical distance [20], the geometry of entanglement has been studied in the case of two qubits [21]. While the mentioned measures address mainly qubits systems, the necessity for noise tolerance and reliability in quantum tasks opened the way to study higher dimensional states, the qudits [22, 23]. In noise-tolerant schemes, magic-state-distillation protocols outperforms their qubits counterparts [24] while a proof of enhanced security for quantum key distribution tasks is derived in [25]. In addition, a recent experimental realisation confirmed the superiority of qudits in certifying entanglement in noisy environments [26]. At the same time, different measure of entanglement for such systems appeared, such as a measure for highly symmetric mixed qudit states [27] and the I concurrence in arbitrary Hilbert space dimensions [28]. Finally, a geometric measure for M-qudit pure states has been proposed in [29].

Following a geometric approach, in the present manuscript, we derive an entanglement monotone [30, 31], *i.e.* a measure of entanglement not increasing under local unitary transformation. This measure can be computed either for pure and mixed states of M-qudit hybrid systems. The measure that we propose i) is invariant under local unitary transformations; ii) has an explicit computable expression; iii) is derived from a tailored form of the Fubini-Study metric. In the specific case of M-qubit systems, the proposed measure iv) has the structure of a distance such that the higher the entanglement of a given state is, the greater is its minimum distance from infinitesimally close states (see Fig. 1); v) in such case the analysis of the eigenvalues of the metric tensor associated with the entanglement measure allows to quantify the robustness of the entanglement of a state and determine if any states are more sensitive to small variations than others.
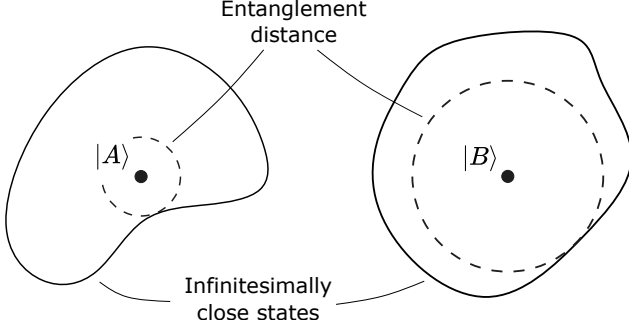
* roberto.franzosi@ino.it

FIG. 1. In the specific case of 2-qubit states, the higher is the entanglement of a state the greater is its minimum distance from infinitesimally close states. In the figure, $|A\rangle$ is a low-entanglement state while $|B\rangle$ is a highly entangled state. In fact, the minimum distance (dashed line) of $|B\rangle$ from infinitesimally closed states (continuous line) is larger than the one associated with $|A\rangle$.

II.   ENTANGLEMENT DISTANCE

A qudit, is a state in a d-dimensional Hilbert space $\mathcal{H}_d$ and a hybrid M-qudit is a state in the tensor product $\mathcal{H} := \mathcal{H}_{d_0} \otimes \mathcal{H}_{d_1} \otimes \cdots \otimes \mathcal{H}_{d_{M-1}}$ of Hilbert spaces of dimension $d_0, d_1, \ldots, d_{M-1}$, respectively. Thus, the dimension of $\mathcal{H}$ is $d = \prod_\mu d_\mu$. First, we derive the entanglement measure for the case of pure hybrid multi-qudit states, then we shall generalize this measure to the case of mixed states.

A.   Pure states

The Hilbert space $\mathcal{H} = \mathcal{H}_{d_0} \otimes \mathcal{H}_{d_1} \otimes \cdots \otimes \mathcal{H}_{d_{M-1}}$ of an hybrid M qudit system carries the Fubini-Study metric [32]

$$\langle d\psi | d\psi \rangle - \frac{1}{4} | \langle \psi | d\psi \rangle - \langle d\psi | \psi \rangle |^2 \,, \tag{1}$$

where $|\psi\rangle$ is a generic normalised state and $|d\psi\rangle$ is an infinitesimal variation of such state. The present study is aimed to endow the Hilbert space with a Fubini Study-like metric that has the desirable property of making it an attractive definition for entanglement measure. For this reason, such distance should not be affected by local operations on single qudits [33, 34]. As a matter of fact, the action of M arbitrary $\mathrm{SU}(d_\mu)$ local unitary operators U_μ ($\mu = 0, \ldots, M-1$) on a given state $|s\rangle$, generates a class of states

$$|U, s\rangle = \prod_{\mu=0}^{M-1} U_\mu |s\rangle \tag{2}$$

that share the same degree of entanglement. For each μ, U_μ operates on the μth qudit of $\mathcal{H}_{d_\mu}$. Thus we define an infinitesimal variation of state (2) as

$$|dU, s\rangle = \sum_{\mu=0}^{M-1} d\tilde{U}_\mu |U, s\rangle \,, \tag{3}$$

where there is no summation on the index μ and each infinitesimal $\mathrm{SU}(d_\mu)$ transformation $d\tilde{U}_\mu$ operates on the μ-th qudit. Such infinitesimal transformation can be written as

$$d\tilde{U}_\mu = -i(\mathbf{n} \cdot \mathbf{T})_\mu d\xi^\mu \tag{4}$$

where $(\mathbf{n} \cdot \mathbf{T})_\mu := \mathbf{n}_\mu \cdot \mathbf{T}_\mu$, $\mathbf{n}_\mu$ is an unit vector in $\mathbb{R}^{d_\mu}$, ξ^μ are real parameters, and where we denote by $T_{\mu a}$, $a = 1, \ldots, d_\mu^2 - 1$, the generators of $\mathfrak{su}(d_\mu)$ algebra (see App. A). From Eq. (1), with this choice, we obtain the following expression for the Fubini-Study metric $g(\mathbf{v})$,

$$\sum_{\mu\nu} g_{\mu\nu}(\mathbf{v}) d\xi^\mu d\xi^\nu = \sum_{\mu\nu} \left(\langle s|(\mathbf{v} \cdot \mathbf{T})_\mu (\mathbf{v} \cdot \mathbf{T})_\nu |s\rangle + \right.$$
$$\left. - \langle s|(\mathbf{v} \cdot \mathbf{T})_\mu |s\rangle \langle s|(\mathbf{v} \cdot \mathbf{T})_\nu |s\rangle \right) d\xi^\mu d\xi^\nu \,. \tag{5}$$

In the latter equation, the real unit vectors $\mathbf{v}_\mu$ are derived by a rotation of the original ones according to

$$\mathbf{v}_\nu \cdot \mathbf{T}_\nu = U_\nu^\dagger \mathbf{n}_\nu \cdot \mathbf{T}_\nu U_\nu \,, \tag{6}$$

where there is no summation on the index ν. Focussing on a generic state $|s\rangle$, for each $\mu = 0, \ldots, M-1$, we obtain from (5)

$$g(\mathbf{v}_\mu)_{\mu\mu} = \sum_{ij} v_{\mu i} v_{\mu j} A_{\mu i j} \,, \tag{7}$$

where the elements of the matrices A_μ, $\mu = 0, \ldots, M-1$, are

$$A_{\mu i j} = \langle s|T_{\mu i} T_{\mu j}|s\rangle - \langle s|T_{\mu i}|s\rangle \langle s|T_{\mu j}|s\rangle \,. \tag{8}$$

The proposed entanglement measure of the state $|s\rangle$ is

$$E(|s\rangle) = \sum_{\mu=0}^{M-1} \left[\mathrm{tr}(A_\mu) - 2(d_\mu - 1) \right] \,. \tag{9}$$

$E(|s\rangle)$ is a proper measure of entanglement satisfying the following properties [11]:

i) The relations (A4) and (A6) make the measure (9) independent from the local operators U_μ. Consequently, its numerical value is associated to the class of states generated by local unitary transformations and not to the specific element chosen inside the class.

ii) From (A4) it results

$$\mathrm{tr}(A_\mu) = \frac{2(d_\mu^2 - 1)}{d_\mu} - \sum_{k=1}^{d_\mu^2 - 1} \langle s|T_{\mu k}|s\rangle^2 \,. \tag{10}$$

Furthermore, the absolute value for the maximum eigenvalue of the set $\{T_{\mu k}\}_k$ is $\sqrt{2(d_\mu - 1)/d_\mu}$ (see App. A), therefore we get

$$\text{tr}(A_\mu) \geq \frac{2(d_\mu^2 - 1)}{d_\mu} - \frac{2(d_\mu - 1)}{d_\mu} \,. \qquad (11)$$

From here,

$$\text{tr}(A_\mu) - 2(d_\mu - 1) \geq 0 \,, \qquad (12)$$

thus,

$$E(|s\rangle) \geq 0 \,. \qquad (13)$$

iii) From (10) we have

$$E(|s\rangle) \leq \sum_{\mu=0}^{M-1} \frac{2(d_\mu - 1)}{d_\mu} \,. \qquad (14)$$

iv) For a maximally entangled state $|s\rangle$,

$$E(|s\rangle) = \sum_{\mu=0}^{M-1} \frac{2(d_\mu - 1)}{d_\mu} \qquad (15)$$

and

$$\langle s|T_{\mu k}|s\rangle = 0 \qquad (16)$$

for each $\mu = 0, \ldots, M - 1$ and $k = 1, \ldots, d_\mu^2 - 1$.

v) For a fully separable state $|s\rangle = |s_0\rangle \otimes \cdots \otimes |s_{M-1}\rangle$ from Eqs. (A5) and (10) we get $E(|s\rangle) = 0$.

In summary, the entanglement measure for a general hybrid qudit state $|s\rangle$, results

$$E(|s\rangle) = \sum_{\mu=0}^{M-1} \left[\frac{2(d_\mu - 1)}{d_\mu} - \sum_{k=1}^{d_\mu^2 - 1} \langle s|T_{\mu k}|s\rangle^2 \right] \,. \qquad (17)$$

Qubit states

Remarkably, in the case of a general M-qubit state $|s\rangle$,

$$\inf_{\{\mathbf{v}_\mu\}_\mu} \text{tr}(g(\mathbf{v})) \qquad (18)$$

identifies a unit vectors $\tilde{\mathbf{v}}_\nu$ for which it results

$$E(|s\rangle) = \text{tr}(g(\tilde{\mathbf{v}})) \,, \qquad (19)$$

where the inf is taken over all the possible orientations of the unit vectors $\mathbf{v}_\mu \in \mathbb{R}^2$. We name entanglement metric (EM) $\tilde{g}$ the Fubini-Study metric associated to $\tilde{\mathbf{v}}_\nu$

$$\tilde{g} = g(\tilde{\mathbf{v}}_\nu) \qquad (20)$$

The off-diagonal elements of $\tilde{g}$ provide the quantum correlations between qubits. In addition, states differing one another for local unitary transformations have the same form of $\tilde{g}$. In this way, the expression of EM identifies the classes of equivalence for M-qubit states.

B. Mixed states

Now, we extend the entanglement measure (9) to the case of mixed states. In order to do so, we require the measure E to satisfy the following 3 conditions [8, 11, 15, 35, 36]:

i) $E(\rho) \geq 0$ and $E(\rho) = 0$ if ρ is fully separable;

ii) $E(\rho)$ is invariant under local unitary transformation, *i.e.* $E(U\rho U^\dagger) = E(\rho)$;

iii) E is a convex functional of the density matrix, that is

$$E(\alpha\rho_1 + (1-\alpha)\rho_2) \leq \alpha E(\rho_1) + (1-\alpha)E(\rho_2) \,, \quad (21)$$

for each $\alpha \in [0,1]$ and mixed states ρ_1 and ρ_2.

Given a mixed state ρ, consider all possible ways of expressing ρ in term of pure states in the form

$$\rho = \sum_j p_j |\psi_j\rangle\langle\psi_j| \,, \qquad (22)$$

where p_j is the probability of measuring the state $|\psi_j\rangle$. We define

$$E(\rho) = min \sum_j p_j E(|\psi_j\rangle) \,, \qquad (23)$$

where the minimum is taken over all the possible combinations of the form (22). The conditions *i)* and *ii)* above, are inherited by $E(\rho)$ since the same properties hold true for $E(|s\rangle)$. Let us verify condition *iii)*. Given $\rho = \alpha\rho_1 + (1-\alpha)\rho_2$, where ρ_1 (ρ_2) can be expressed in the form $\sum_j p_j^1 |\psi_j^1\rangle\langle\psi_j^1|$ ($\sum_j p_j^2 |\psi_j^2\rangle\langle\psi_j^2|$) in several ways. We have $\rho = \sum_j (\alpha p_j^1 |\psi_j^1\rangle\langle\psi_j^1| + (1-\alpha)p_j^2 |\psi_j^2\rangle\langle\psi_j^2|)$, thus

$$\min_{\{p^1,|\psi^1\rangle,p^2,|\psi^2\rangle\}} \sum_j (\alpha p_j^1 E(|\psi_j^1\rangle) + (1-\alpha)p_j^2 E(|\psi_j^2\rangle) \leq$$

$$\min_{\{p^1,|\psi^1\rangle\}} \sum_j \alpha p_j^1 E(|\psi_j^1\rangle) + \min_{\{p^2,|\psi^2\rangle\}} \sum_j (1-\alpha)p_j^2 E(|\psi_j^2\rangle)$$

$$(24)$$

since the minimum of a set is always less or equal to the minimum of its subsets.

III. EXAMPLES OF APPLICATION

In order to verify the efficacy of the proposed entanglement measure, we have first considered two families of one-parameter multi-qubit states depending on a real parameter. The degree of entanglement of each state depends on this parameter and the configuration corresponding to maximally entangled states for each of the families considered is known. The first family of states we consider in III A, III A 1 and III A 2, has been introduced by Briegel and Raussendorf in Ref. [13], for this

reason we will name the elements in this family Briegel-Raussendorf states (BRS). The second family of states, in III B, is related to the Greenberger-Horne-Zeilinger states [37], since it contains one of these states. We will name the elements of such family Greenberger-Horne-Zeilinger–like states (GHZLS). It is worth emphasizing that in Ref. [13] it has been shown that the maximally entangled states of these two families are not equivalent if $M \geq 4$, whereas they are equivalent if $M \leq 3$, where M is the number of qubits considered. This fact offers us a further test for our approach to entanglement estimation. In fact, we have found that $i)$ the entanglement measure (9) provides the same value for the maximally entangled states of both families; $ii)$ in the case $M \leq 3$, the entanglement metric (20) has the same form for the maximally entangled states of the two families, whereas for $M \geq 4$ the EMs of the maximally entangled states of the two families are inequivalent. In Sec. III C, we have considered a family of three-qubit states depending on two real parameters. With a suitable choice of these parameters, the state can be fully separable or bi-separable, whereas in the generic case it is a genuine tripartite entangled state. We will show that the proposed entanglement measure provides an accurate description of all these cases. In Sec. III D we have applied the entanglement measure (9) to the case of an hybrid qudit system and in Sec. III E to the case of two qutrits.

A.   Briegel Raussendorf states

In the case of qubit, the generators $\mathbf{T}_\mu$ are the Pauli matrices $\boldsymbol{\sigma}_\mu$. We denote with $\Pi_0^\mu = (\mathbb{I} + \sigma_{\mu 3})/2$ and $\Pi_1^\mu = (\mathbb{I} - \sigma_{\mu 3})/2$ the projector operators onto the eigenstates of $\sigma_{\mu 3}$, $|0\rangle_\mu$ (with eigenvalue $+1$) and $|1\rangle_\mu$ (with eigenvalue -1), respectively. Each M-qubit state of the BRS class is derived by applying to the fully separable state

$$|r,0\rangle = \bigotimes_{\mu=0}^{M-1} \frac{1}{\sqrt{2}}(|0\rangle_\mu + |1\rangle_\mu) \,, \qquad (25)$$

the non-local unitary operator

$$U_0(\phi) = \exp(-i\phi H_0) = \prod_{\mu=1}^{M-1} \left(\mathbb{I} + \alpha \Pi_0^\mu \Pi_1^{\mu+1} \right) \,, \quad (26)$$

where $H_0 = \sum_{\mu=1}^{M-1} \Pi_0^\mu \Pi_1^{\mu+1}$ and $\alpha = (e^{-i\phi} - 1)$. The full operator (26) is diagonal on the states of the standard basis $\{|0\cdots 0\rangle, |0\cdots 01\rangle, \ldots, |1\cdots 1\rangle\}$. In fact, each vector of the latter basis is identified by M integers $n_0, \ldots, n_{M-1} = 0,1$ as $|\{n\}\rangle = |n_{M-1}\, n_{M-2}\ \ n_0\rangle$ and we can enumerate such vectors according to the binary integers representation $|k\rangle = |\{n^k\}\rangle$, with $k = \sum_{\mu=0}^{M-1} n_\mu^k 2^\mu$,

where n_ν^k is the ν-th digit of the number k in binary representation and $k = 0, \ldots, 2^M - 1$. Then, the eigen-

value λ_k of operator (26), corresponding to a given eigenstate $|k\rangle$ of this basis, results

$$\lambda_k = \sum_{j=0}^{n(k)} \binom{n(k)}{j} \alpha^j \,, \qquad (27)$$

where $n(k)$ is the number of ordered couples 01 inside the sequence of the base vector $|k\rangle$. For the initial state (25) we consistently get

$$|r,0\rangle_M = 2^{-M/2} \sum_{k=0}^{2^M-1} |k\rangle \,, \qquad (28)$$

and, under the action of $U_0(\phi)$, one obtains

$$|r,\phi\rangle_M = 2^{-M/2} \sum_{k=0}^{2^M-1} \sum_{j=0}^{n(k)} \binom{n(k)}{j} \alpha^j |k\rangle \qquad (29)$$

For $\phi = 2\pi k$, with $k \in \mathbb{Z}$, this state is separable, whereas, for all the other choices of the value ϕ, it is entangled. In particular, in [13] it is argued that the values $\phi = (2k+1)\pi$, where $k \in \mathbb{Z}$, give maximally entangled states.

1.   Fubini-Study metric for the Briegel Raussendorf states $M = 2, 3$

In the case of two-qubit BRS, the trace of the Fubini-Study metric is

$$\mathrm{tr}(g) = \sum_{\nu=0}^{1} \left[1 - c^2 \left(c v_{\nu 1} + (-1)^{\nu+1} s v_{\nu 2} \right)^2 \right] \,, \qquad (30)$$

where $c = \cos(\phi/2)$ and $s = \sin(\phi/2)$. (30) is minimised with the choice $\tilde{\mathbf{v}}_\nu = \pm(c, (-1)^{\nu+1}s, 0)$. Consistently, the EM results in

$$\tilde{g} = \begin{pmatrix} s^2 & 1 \\ 1 & s^2 \end{pmatrix} \qquad (31)$$

and

$$E(|r,\phi\rangle_2) = 2s^2 \,. \qquad (32)$$

In the case $M = 3$ and $\phi \neq (2k+1)\pi$, with $k \in \mathbb{Z}$, the trace of g,

$$\mathrm{tr}(g) = \left[3 - c^2 \left(c(v_{01} + v_{11} + v_{21}) + s(v_{22} - v_{02}) \right)^2 \right] \,, \qquad (33)$$

is minimised with the choices $\tilde{\mathbf{v}}_0 = (c, -s, 0)$, $\tilde{\mathbf{v}}_1 = (1, 0, 0)$ and $\tilde{\mathbf{v}}_2 = (c, s, 0)$. The EM and the entanglement measure in this case result to be

$$\tilde{g} = s^2 \begin{pmatrix} 1 & c & -2s^2 c^2 \\ c & 1+c^2 & c \\ -2s^2 c^2 & c & 1 \end{pmatrix} \qquad (34)$$

and

$$E(|r, \phi\rangle_3) = s^2 \left(3 + c^2\right), \qquad (35)$$

respectively. By direct calculation, one can verify that in the case of the maximally entangled BRS ($\phi = (2k+1)\pi$, $k \in \mathbb{Z}$), the choice $\mathbf{v}_0 = (-1, 0, 0)$, $\mathbf{v}_1 = (0, 0, 1)$ and $\mathbf{v}_2 = (1, 0, 0)$ minimizes $\text{tr}(g)$ and the corresponding EM is the 3×3 matrix of ones.

2. Fubini-Study metric for the Briegel Raussendorf states $M > 3$

For a general M-qubit state $|r, \phi\rangle_M$, the trace of g results

$$\text{tr}(g) = \left\{ M - \sum_{\nu=0}^{M-1} [v_{\nu 3} w_{\nu 3} + v_{\nu+} w_{\nu-} + v_{\nu-} w_{\nu+}]^2 \right\}, \qquad (36)$$

where $v_{\nu\pm} = v_{\nu 1} \pm i v_{\nu 2}$, $c_k = 2^{-M/2} \lambda_k$, and

$$\begin{aligned} w_{\nu-} &= \sum_{k=0}^{2^M-1} \delta_{n_\nu^k, 0} c_{k+2^\nu}^* c_k, \\ w_{\nu+} &= \sum_{k=0}^{2^M-1} \delta_{n_\nu^k, 1} c_{k-2^\nu}^* c_k, \\ w_{\nu 3} &= \sum_{k=0}^{2^M-1} (-1)^{n_\nu^k} |c_k|^2. \end{aligned} \qquad (37)$$

The trace is minimised by setting $\tilde{v}_{\nu+} = w_{\nu-}^\star / \|\mathbf{w}_\nu\|$, $\tilde{v}_{\nu-} = w_{\nu+}^\star / \|\mathbf{w}_\nu\|$ and $\tilde{v}_{\nu 3} = w_{\nu 3} / \|\mathbf{w}_\nu\|$.

From the latter, we get the entanglement measure for the BRS

$$E(|r, \phi\rangle_M) = \left(M - \sum_{\nu=0}^{M-1} \|\mathbf{w}_\nu\|^2 \right). \qquad (38)$$

B. Greenberger-Horne-Zeilinger–like states

Now, we consider a second class of M-qubit states, the GHZLS, defined according to

$$|GHZ, \theta\rangle_M = \cos(\theta)|0\rangle + \sin(\theta)e^{i\varphi}|2^M - 1\rangle. \qquad (39)$$

For $\theta = k\pi/2$ and $\forall \varphi$, where $k \in \mathbb{Z}$, these states are fully separable, whereas $\theta = k\pi/2 + \pi/4$ ($\forall \varphi$) selects the maximally entangled states. In this case, the trace for the Fubini-Study metric,

$$\text{tr}(g) = M - \cos^2(2\theta) \sum_{\nu=0}^{M-1} (v_{\nu 3})^2, \qquad (40)$$

is minimised by the values $v_{\nu 3} = 1$. Consistently, we have

$$\tilde{g} = \sin^2(2\theta) J_M \qquad (41)$$

where J_M is the $M \times M$ matrix of ones. The entanglement measure for the GHZLS results

$$E(|GHZ, \theta\rangle_M) = M \sin^2(2\theta). \qquad (42)$$

We have mentioned above that in the case $M = 2, 3$, the maximally-entangled BRS $|r, 2\pi k + \pi\rangle$, where $k \in \mathbb{Z}$ and the maximally entangled GHZLS are equivalent because differing just for local unitary transformations. In the present approach, this equivalence is caught by the entanglement matrices. We have shown that, in the case $M = 2, 3$, the EM for the maximally entangled states belonging to these two families are identical. Furthermore, we have verified for some cases with $M > 3$, that the EMs for the maximally entangled states of the two families are different thus confirming the results of Ref. [13].

C. Three-qubit states depending on two parameters

The last class of qubit states we consider is

$$\begin{aligned} |\varphi, \gamma, \tau\rangle_3 = &\cos(\gamma)|0\rangle[\cos(\tau)|00\rangle + \sin(\tau)|11\rangle] \\ &+ \sin(\gamma)|1\rangle[\sin(\tau)|00\rangle + \cos(\tau)|11\rangle]. \end{aligned} \qquad (43)$$

These states are fully separable for $\gamma = 0, \pi/2$ and $\tau = 0, \pi/2$ whereas they are bi-separable for $\tau = \pi/4$. In this case, the trace of the Fubini-Study metric is

$$\begin{aligned} \text{tr}(g) = &\{3 - \cos^2(2\gamma)\cos^2(2\tau)[(v_{03})^2 + (v_{13})^2] \\ &- [\sin(2\gamma)\sin(2\tau)v_{21} + \cos(2\gamma)v_{23}]^2\} \end{aligned} \qquad (44)$$

and it is minimised by the values $\tilde{\mathbf{v}}_{\nu 3} = (0, 0, 1)$, $\nu = 0, 1$ and

$$\begin{aligned} \tilde{v}_{31} &= \frac{\sin(2\gamma)\sin(2\tau)}{\sqrt{\sin^2(2\gamma)\sin^2(2\tau) + \cos^2(2\gamma)}}, \\ \tilde{v}_{32} &= 0, \\ \tilde{v}_{33} &= \frac{\cos(2\gamma)}{\sqrt{\sin^2(2\gamma)\sin^2(2\tau) + \cos^2(2\gamma)}}. \end{aligned} \qquad (45)$$

Consistently, the entanglement measure for these states results to be

$$E(|\varphi, \gamma, \tau\rangle_3) = [2\sin^2(2\tau) + 3\sin^2(2\gamma)\cos^2(2\tau)]. \qquad (46)$$

D. Hybrid two-qudit states depending on one parameter

As an example of application to hybrid qudit systems, we consider the Hilbert space $\mathcal{H} = \mathcal{H}_2 \otimes \mathcal{H}_3$, i.e. the product of qubit and qutrit states. Let us denote the elements of a basis in such Hilbert space with $|\alpha, j\rangle$, where $\alpha = \pm$ and $j = 0, 1, 2$ and consider the following family of single-parameter states

$$|s, \theta\rangle = \cos(\theta)|+, 0\rangle + \sin(\theta)|-, 2\rangle. \qquad (47)$$

We expect the state with a higher degree of entanglement will correspond to $\theta = \pi/4$. Note that this is not a

maximally entangled state since the component $|1\rangle$ of the second Hilbert space is absent. From Eq. (8), we have

$$A_0 = \begin{pmatrix} 1 & i\cos(2\theta) & 0 \\ -i\cos(2\theta) & 1 & 0 \\ 0 & 0 & 1 - \cos^2(2\theta) \end{pmatrix}. \quad (48)$$

In the case of qutrits, the generators $\mathbf{T}_\mu$ can be represented with the Gell-Mann matrices. By direct calculation, one can verify that the only non-null matrix elements for A_1 are the following

$$(A_1)_{11} = \cos^2(\theta),$$
$$(A_1)_{22} = \cos^2(\theta),$$
$$(A_1)_{33} = \cos^2(\theta)\sin^2(\theta),$$
$$(A_1)_{44} = \sin^2(\theta),$$
$$(A_1)_{55} = \sin^2(\theta),$$
$$(A_1)_{66} = 3\cos^2(\theta)\sin^2(\theta),$$
$$(A_1)_{77} = 1,$$
$$(A_1)_{88} = 1.$$

Thus, from Eq. (17) we have

$$E(|s,\theta\rangle) = 2\sin^2(2\theta). \quad (49)$$

In (49), $\theta = \pi/4$ provides the maximally entangled state.

In the next section, we will compare entanglement measure $E(|s,\theta\rangle)/2$ with the von Neumann entropy

$$\mathcal{E}(\rho(\theta)) = -\cos^2(\theta)\log_2(\cos^2(\theta)) - \sin^2(\theta)\log_2(\sin^2(\theta)) \quad (50)$$

of the density matrix $\rho(\theta) = |s,\theta\rangle\langle s,\theta|$ associated to the same state.

E. M-qudit states depending on two parameters

Let us consider an M-qutrit system, that has a Hilbert space $\mathcal{H} = \mathcal{H}_3 \otimes \cdots \otimes \mathcal{H}_3$, that is to say, the product of M qutrit states. We have considered the following generalisation of the GHZLS states to qutrits,

$$|s,\theta,\phi\rangle_M = \sin(\theta)\cos(\phi)|0,\ldots,0\rangle + \sin(\theta)\sin(\phi)|1,\ldots,1\rangle + \cos(\theta)|2,\ldots,2\rangle, \quad (51)$$

which is a family of 2-parameter states. We have,

$$(A_\mu)_{11} = \sin^2(\theta),$$
$$(A_\mu)_{22} = \sin^2(\theta),$$
$$(A_\mu)_{33} = \frac{1}{4}\sin^2(\theta)\left(3 + \cos(2\theta) - 2\sin^2(\theta)\cos(4\phi)\right),$$
$$(A_\mu)_{44} = \sin^2(\theta)\sin^2(\phi) + \cos^2(\theta),$$
$$(A_\mu)_{55} = \sin^2(\theta)\sin^2(\phi) + \cos^2(\theta),$$
$$(A_\mu)_{66} = 3\sin^2(\theta)\cos^2(\theta),$$
$$(A_\mu)_{77} = \sin^2(\theta)\cos^2(\phi) + \cos^2(\theta),$$
$$(A_\mu)_{88} = \sin^2(\theta)\cos^2(\phi) + \cos^2(\theta),$$

for $\mu = 0, \ldots, M-1$. Thus, it results

$$E(|s,\theta,\phi\rangle_M) = \frac{M}{4}\sin^2(\theta)\big(9 + 7\cos(2\theta) - 2\sin^2(\theta)\cos(4\phi)\big). \quad (52)$$

In the next section we compare the entanglement measure $E(|s,\theta,\phi\rangle_M)/M$ of the states (51) with the von Neumann entropy

$$\mathcal{E}(\rho(\theta,\phi)) = -a^2\log_2(a^2) - b^2\log_2(b^2) - c^2\log_2(c^2), \quad (53)$$

where $\rho(\theta,\phi) = |s,\theta,\phi\rangle_{22}\langle s,\theta,\phi|$ is the density matrix associated with the same states in the case $M = 2$. Here, $a = \sin(\theta)\cos(\phi)$, $b = \sin(\theta)\sin(\phi)$ and $c = \cos(\theta)$.

IV. RESULTS

A. Entanglement measure

In Fig. 2, we plot the measure $E(|r,\phi\rangle_M)/M$ vs $\phi/(2\pi)$ according to Eq. (38), for the multi-qubit states (29) in the case $M = 3, 4, 7, 9$. Figure 2 shows that the proposed entanglement measure provides a correct estimation of the degree of entanglement for the BRS in all the cases considered. In particular, for the fully separable states ($\phi = 0, 2\pi$), it is zero, whereas, for the maximally entangled states ($\phi = \pi$), it provides the maximum possible value for the trace, that is $E(|r,\pi\rangle_M)/M = 1$. This implies that the expectation values on the maximally entangled states of the operators $\tilde{\mathbf{v}}_\nu \cdot \boldsymbol{\sigma}_\nu$ ($\nu = 0, \ldots, M-1$) are zero.

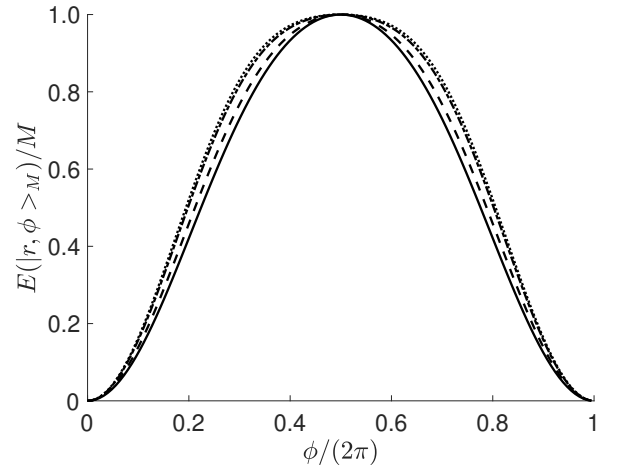
FIG. 2. The figure reports the entanglement measure $E(|r,\phi\rangle_M)/M$ vs $\phi/(2\pi)$ for the states (29) in the cases $M = 3$ (continuous line), $M = 4$ (dashed line), $M = 7$ (dot-dashed line) and $M = 9$ (dotted line).

The entanglement measure (9) successfully passes also the second test of the GHZLS for which it provides zero

in the case of fully separable states ($\theta = 0, \pi$), and the maximum value (that is 1) in the case of the maximally entangled state ($\theta = \pi/2$). In figure 3, we compare the curves $E(|r, \phi\rangle_M)/M$ vs $\phi/(2\pi)$ in continuous line and $E(|GHZ, \theta\rangle_M)/M$ vs $2\theta/\pi$ in dashed line, for the case $M = 3$. Even in this case, the expectation values of the operators $\tilde{\mathbf{v}}_\nu \cdot \boldsymbol{\sigma}_\nu$ ($\nu = 0, \ldots, M-1$) on the maximally entangled states are zero.
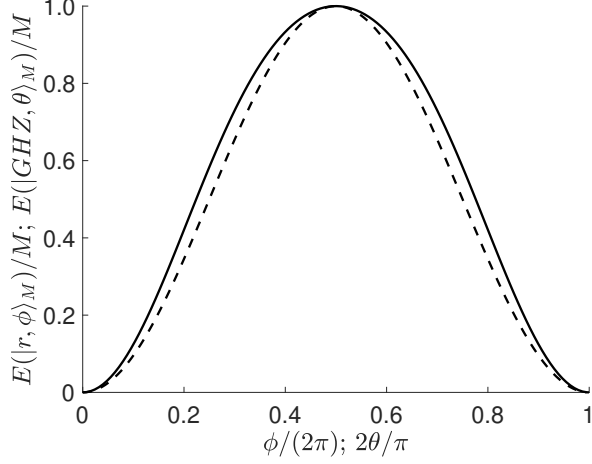

FIG. 3. In this figure we compare the entanglement measures $E(|r, \phi\rangle_M)/M$ vs $\phi/(2\pi)$ for the states (29) in continuous line, and $E(|GHZ, \theta\rangle_M)/M$ vs $2\theta/\pi$ for the states (39) in dashed line, for the case $M = 3$.

In Fig. 4, we report in a 3D plot the measure $E(|\varphi, \gamma, \tau\rangle_3)/3$ as a function of γ/π and τ/π according to Eq. (46), for the states (43). The measure (9) catches

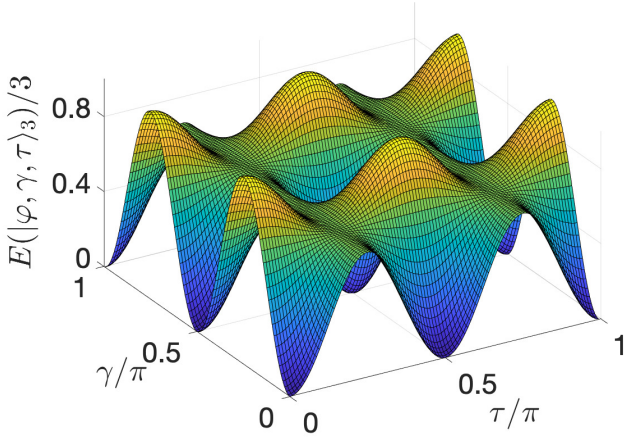FIG. 4. The figure reports the three dimensional plot of the entanglement measure $E(|\varphi, \gamma, \tau\rangle_3)/3$ as a function of γ/π and τ/π for the states (43).

in a surprisingly clear way the entanglement properties

of this family of states. In particular, $E(|\varphi, \gamma, \tau\rangle_3)/3$ is null in the case of fully separable states ($\gamma = 0, \pi/2, \pi$ and $\tau = 0, \pi/2, \pi$) and it is maximum (with value 1) in the case of maximally entangled states ($\gamma = \pi/4, 3\pi/4$ and $\tau = 0, \pi/2, \pi$). In addition, the case of bi-separable states ($\tau = \pi/4$) results in $0 < E(|\varphi, \gamma, \tau\rangle_3)/3 < 1$.

Figure 5 refers to the hybrid two-qudit states (47). Here, we compare the curves of entanglement measure $E(|s, \theta\rangle)/2$ vs θ/π of states (47) in a continuous line, and the von Neumann entropy $\mathcal{E}(|s, \theta\rangle)$ vs θ/π in dashed line, for the same states. This figure clearly shows that, although these two curves are different, they strongly agree in the quantification of the entanglement of the different states. Note that the highly entangled state associated with $\theta = \pi/4$ has an entanglement measure of 1, lower than the maximally entangled state of this Hilbert space which, using (15), report a value of 7/6.
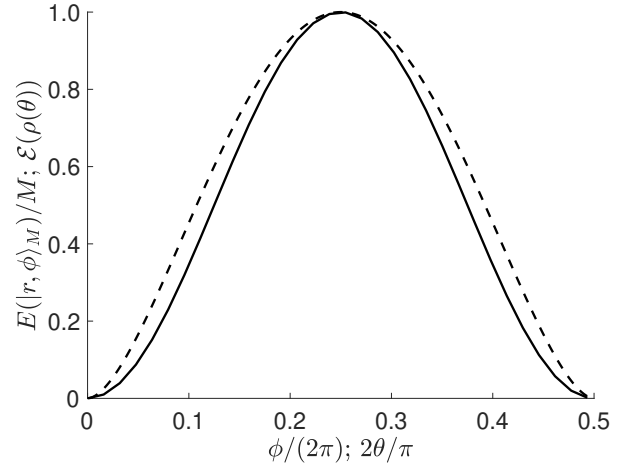

FIG. 5. The figure compares the entanglement measure $E(|r, \phi\rangle_M)/M$ vs $\phi/(2\pi)$ in continuous line for the hybrid two-qudit states (47), and the von Neumann entropy $\mathcal{E}(\rho(\theta))$ vs θ/π in dashed line for the same states.

In Fig. 6, we report the entanglement measure $E(|s, \theta, \phi\rangle_M)/M$ as a function of θ/π and ϕ/π given in Eq. (52), for the multi-qubit states (51). Even in this example, the measure (9) catches in a surprisingly clear way the entanglement properties of this family of multi-qudit states. In particular, $E(|s, \theta, \phi\rangle_M)/M$ is null in the case of fully separable states, i.e. for $\theta = 0$, $\forall \phi$ and $\theta = \pi/2, \phi = 0, \pi/2, \pi$. In case of $\phi = 0, \pi$, the entanglement measure changes over θ and shows local maximum for $\theta = \pi/4$. For $\theta = \pi/2$, the measure changes over ϕ displaying local maxima for $\phi = \pi/4, 3\pi/4$. Furthermore, the state corresponding to $\sin(\theta)\cos(\phi) = \sin(\theta)\sin(\phi) = \cos(\theta) = 1/\sqrt{3}$ is a maximally entangled state to which corresponds an entanglement measure (15) of value 4/3.

In Fig. 7, we report the 3D plot for the von Neumann entropy $\mathcal{E}(\rho(\theta, \phi))$ (see Eq. (53)) as a function of θ/π and ϕ/π. The entropy is calculated for the density ma-
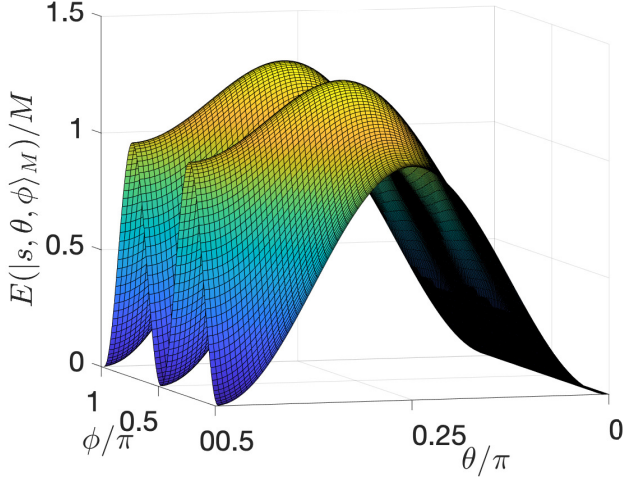
FIG. 6. The plot shows the entanglement measure $E(|s, \theta, \phi\rangle_M)/M$ in (52) as a function of θ/π and ϕ/π for the states (51).

trix $\rho(\theta, \phi) = |s, \theta, \phi\rangle_{22}\langle s, \theta, \phi|$ associated to the family of two-qudit states (51). The comparison between the
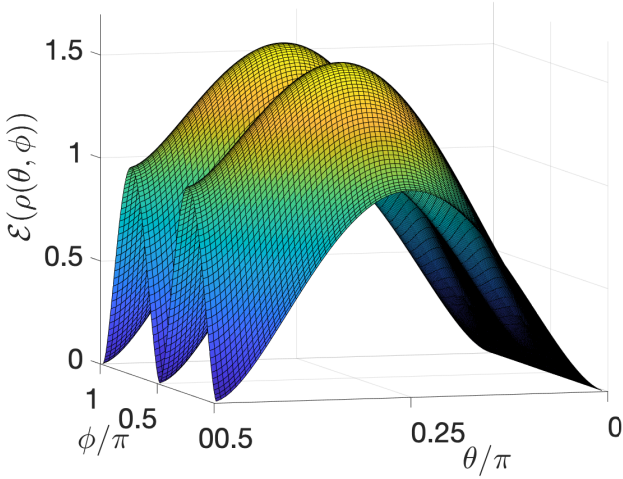

FIG. 7. The figure shows $\mathcal{E}(\rho(\theta, \phi))$ as a function of θ/π and ϕ/π given in Eq. (53). The density matrix is associated with the states (51), $\rho(\theta, \phi) = |s, \theta, \phi\rangle_{22}\langle s, \theta, \phi|$ in the case $M = 2$.

figures 6 and 7 clearly shows that, although the functions $E(|s, \theta, \phi\rangle_M)/M$ and $\mathcal{E}(\rho(\theta, \phi))$ are different, they fully agree, in the entanglement estimation, for the states $|s, \theta, \phi\rangle$.

B. Eigenvalues analysis for M-qubit states

In the case of multi-qubit states, a further interesting characteristics of the entanglement measure comes

from the analysis of the entanglement metric's eigenvalues. In fig. 8, we compare the plots of the eigenvalues of $\tilde{g}$ for $|r, \phi\rangle_M$ vs $\phi/(2\pi)$ (dotted lines), with the plot of the unique not vanishing eigenvalue of $\tilde{g}$ for GHZLS vs $2\theta/\pi$ (continuous line), in the case $M = 7$. When
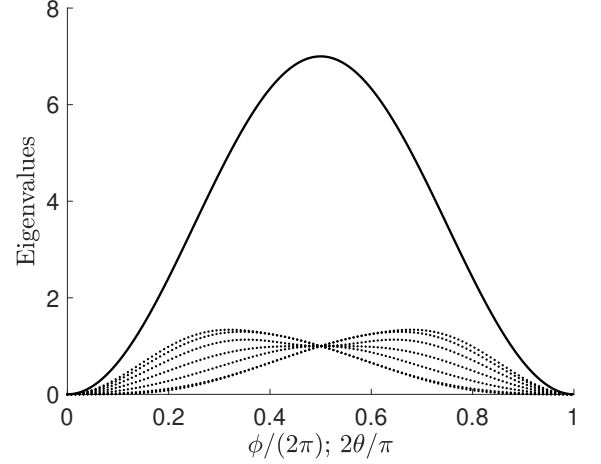

FIG. 8. Plot of the $\tilde{g}$ eigenvalues for the state $|r, \phi\rangle_M$ vs $\phi/(2\pi)$ in dotted lines and the unique not vanishing eigenvalue of $\tilde{g}$ for the state GHZLS vs $2\theta/\pi$ in continuous line, for the case $M = 7$.

$\phi \neq 0, 2\pi$ the EM of the BRS, $\tilde{g}$, has exactly M non-zero eigenvalues. On the other hand, the GHZLS have only one non-vanishing eigenvalue. Although the value of the latter is greater than the eigenvalues of the BRS (see Fig. 8), the GHZLS appear weak, in the sense of entanglement, since there exist $M - 1$ directions with null minimum distance between states. This fact makes the class of the BRS robust in the sense of entanglement. In fact, the minimum distance between states in a random direction is greater than the minimum eigenvalue of the metric and, therefore, greater than zero.

Within the scenario that we have proposed, the entanglement has the physical interpretation of an obstacle to the minimum distance between infinitesimally close states. In fact, by defining the distance between a given state represented by the vector $|U, s\rangle$ and an infinitesimally close state associated with the vector $|dU, s\rangle$ as $ds^2 = \text{tr}(g(\mathbf{v}))dr^2$ where $\sum_\mu (d\xi^\mu)^2 = dr^2$, it results

$$ds^2 \geq E(|s\rangle)dr^2. \tag{54}$$

This shows that the minimum distance density ds^2/dr^2, obtained by varying the vectors $\mathbf{v}$, is bounded from below by the entanglement measure $E(|s\rangle)$. For fully separable states, the minimum distance density is zero whereas, for maximally entangled states, it results M at the very best. Finally, from the analysis of the eigenvalues we can investigate the sensitivity of different states to small variations. Fig. 9 shows that at different points in pa-
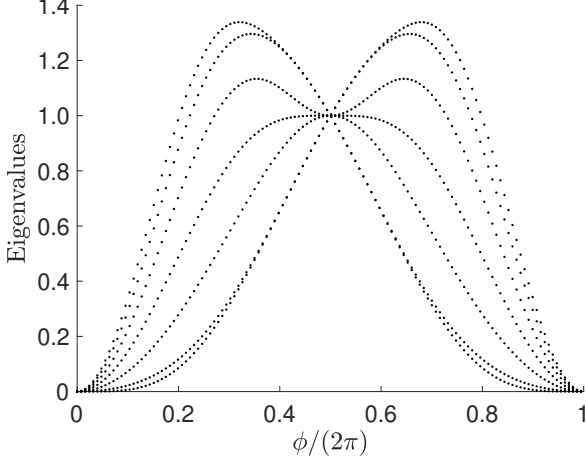
FIG. 9. The figure plots the $\tilde{g}$ eigenvalues for the state $|r, \phi\rangle_M$ vs $\phi/(2\pi)$ for the case $M = 7$.

rameter space corresponds different state sensitivity of $|r, \phi\rangle_7$. For instance, if we move out of $\phi = \pi/2$, following the eigenvector's direction corresponding to the maximum eigenvalue of $\tilde{g}$, we find a greater distance than moving along the eigenvector's of the maximally entangled state at $\phi = \pi$. Such analysis can be profitably used within quantum metrology applications.

Appendix A: Generalized Gell-Mann matrices

As fundamental representation for the generators of the algebra of $SU(d_\mu)$, we use the generalized Gell-Mann matrices. These are the following $d_\mu^2 - 1$, $d_\mu \times d_\mu$ matrices. Let $E_{j,k}$ (for $j, k = 1, \ldots, d_\mu$) be the matrix with 1 as (j, k)-th entry and 0 elsewhere. We define

$$T_{\mu\ell} = (E_{j,k} + E_{k,j}), \qquad (A1)$$

where $\ell = 2(k-j)+(j-1)(2d_\mu-j)-1$ for $j = 1, \ldots, d_\mu-1$, $k = j + 1, \ldots, d_\mu$,

$$T_{\mu\ell} = -i(E_{j,k} - E_{k,j}), \qquad (A2)$$

where $\ell = 2(k-j)+(j-1)(2d_\mu-j)$ for $j = 1, \ldots, d_\mu-1$, $k = j + 1, \ldots, d_\mu$ and

$$T_{\mu\ell} = \left[\sum_{j=1}^{k} E_{j,j} - kE_{k+1,k+1}\right] \sqrt{\frac{2}{k(k+1)}}, \qquad (A3)$$

where $\ell = d_\mu(d_\mu - 1) + k$ for $k = 1, \ldots, d_\mu - 1$. In the case $d_\mu = 2$, these generators are given in terms of the Pauli matrices according to $T_{\mu1} = \sigma_{\mu1}$, $T_{\mu2} = \sigma_{\mu2}$ and $T_{\mu3} = \sigma_{\mu3}$. In the case $d_\mu = 3$, the generators are given by the standard Gell-Mann matrices.

In the general case, the following identity holds true,

$$\sum_{k=1}^{d_\mu^2-1} T_{\mu k}T_{\mu k} = \frac{2(d_\mu^2 - 1)}{d_\mu}\mathbb{I} \qquad (A4)$$

and, for each normalized state $|s_\mu\rangle \in \mathcal{H}_{d_\mu}$, it results

$$\sum_{k=1}^{d_\mu^2-1} \langle s_\mu|T_{\mu k}|s_\mu\rangle^2 = \frac{2(d_\mu - 1)}{d_\mu}. \qquad (A5)$$

For each normalized state $|s\rangle \in \mathcal{H}$ and unitary local operator $U_\mu : \mathcal{H}_{d_\mu} \to \mathcal{H}_{d_\mu}$, it results

$$
\begin{aligned}
&\sum_{k=1}^{d_\mu^2-1} \langle s|U_\mu^\dagger T_{\mu_k} U_\mu|s\rangle^2 = \\
&\sum_{k=1}^{d_\mu^2-1} \sum_{\alpha=1}^{d_\mu^2-1} (n_\alpha^k)^2 \langle s|T_{\mu\alpha}|s\rangle^2 = \\
&\sum_{\alpha=1}^{d_\mu^2-1} \langle s|T_{\mu\alpha}|s\rangle^2 \sum_{k=1}^{d_\mu^2-1} (n_\alpha^k)^2 = \\
&\sum_{\alpha=1}^{d_\mu^2-1} \langle s|T_{\mu\alpha}|s\rangle^2.
\end{aligned} \qquad (A6)
$$

[1] O. Gühne and G. Toth, Entanglement detection, Physics Reports **474**, 1 (2009).

[2] F. Arute, K. Arya, R. Babbush, D. Bacon, J. C. Bardin, R. Barends, R. Biswas, S. Boixo, F. G. Brandao, D. A. Buell, *et al.*, Quantum supremacy using a programmable superconducting processor, Nature **574**, 505 (2019).

[3] J. Sperling and I. A. Walmsley, Entanglement in macroscopic systems, Phys. Rev. A **95**, 062116 (2017).

[4] V. Giovannetti, S. Mancini, D. Vitali, and P. Tombesi, Characterizing the entanglement of bipartite quantum systems, Phys. Rev. A **67**, 022320 (2003).

[5] R. Horodecki, P. Horodecki, M. Horodecki, and K. Horodecki, Quantum entanglement, Rev. Mod. Phys. **81**, 865 (2009).

[6] S. Popescu and D. Rohrlich, Thermodynamics and the measure of entanglement, Phys. Rev. A **56**, R3319 (1997).

[7] W. K. Wootters, Entanglement of formation of an arbitrary state of two qubits, Phys. Rev. Lett. **80**, 2245 (1998).

[8] C. H. Bennett, D. P. DiVincenzo, J. A. Smolin, and W. K. Wootters, Mixed-state entanglement and quantum error correction, Phys. Rev. A **54**, 3824 (1996).

[9] C. H. Bennett, G. Brassard, S. Popescu, B. Schumacher, J. A. Smolin, and W. K. Wootters, Purification of noisy entanglement and faithful teleportation via noisy channels, Phys. Rev. Lett. **76**, 722 (1996).

[10] M. Horodecki, P. Horodecki, and R. Horodecki, Mixed-state entanglement and distillation: Is there a "bound" entanglement in nature?, Phys. Rev. Lett. **80**, 5239 (1998).

[11] V. Vedral, M. B. Plenio, M. A. Rippin, and P. L. Knight, Quantifying entanglement, Phys. Rev. Lett. **78**, 2275 (1997).

[12] W. Dür, G. Vidal, and J. I. Cirac, Three qubits can be entangled in two inequivalent ways, Phys. Rev. A **62**, 062314 (2000).

[13] H. J. Briegel and R. Raussendorf, Persistent entanglement in arrays of interacting particles, Phys. Rev. Lett. **86**, 910 (2001).

[14] V. Coffman, J. Kundu, and W. K. Wootters, Distributed entanglement, Phys. Rev. A **61**, 052306 (2000).

[15] J. Eisert and H. J. Briegel, Schmidt measure as a tool for quantifying multiparticle entanglement, Phys. Rev. A **64**, 022306 (2001).

[16] A. R. R. Carvalho, F. Mintert, and A. Buchleitner, Decoherence and multipartite entanglement, Phys. Rev. Lett. **93**, 230501 (2004).

[17] L. Pezzé and A. Smerzi, Entanglement, nonlinear dynamics, and the heisenberg limit, Phys. Rev. Lett. **102**, 100401 (2009).

[18] P. Hyllus, W. Laskowski, R. Krischek, C. Schwemmer, W. Wieczorek, H. Weinfurter, L. Pezzé, and A. Smerzi, Fisher information and multiparticle entanglement, Phys. Rev. A **85**, 022321 (2012).

[19] S. Scali and R. Franzosi, Entanglement estimation in non-optimal qubit states, Annals of Physics **411**, 167995 (2019).

[20] S. L. Braunstein and C. M. Caves, Statistical distance and the geometry of quantum states, Phys. Rev. Lett. **72**, 3439 (1994).

[21] P. Levay, The geometry of entanglement: metrics, connections and the geometric phase, Journal of Physics A: Mathematical and General **37**, 1821 (2004).

[22] F. S. Khan and M. Perkowski, Synthesis of multi-qudit hybrid and d-valued quantum logic circuits by decomposition, Theoretical Computer Science **367**, 336 (2006).

[23] K. Kreis and P. van Loock, Classifying, quantifying, and witnessing qudit-qumode hybrid entanglement, Phys. Rev. A **85**, 032307 (2012).

[24] E. T. Campbell, H. Anwar, and D. E. Browne, Magic-state distillation in all prime dimensions using quantum reed-muller codes, Phys. Rev. X **2**, 041021 (2012).

[25] L. Sheridan and V. Scarani, Security proof for quantum key distribution using qudit systems, Phys. Rev. A **82**, 030301 (2010).

[26] S. Ecker, F. Bouchard, L. Bulla, F. Brandt, O. Kohout, F. Steinlechner, R. Fickler, M. Malik, Y. Guryanova, R. Ursin, and M. Huber, Overcoming noise in entanglement distribution, Phys. Rev. X **9**, 041042 (2019).

[27] A. Barasiński and M. Nowotarski, Quantifying entanglement properties of qudit mixed states with incomplete permutation symmetry, Phys. Rev. A **95**, 042333 (2017).

[28] P. Rungta, V. Bužek, C. M. Caves, M. Hillery, and G. J. Milburn, Universal state inversion and concurrence in arbitrary dimensions, Phys. Rev. A **64**, 042315 (2001).

[29] A. S. M. Hassan and P. S. Joag, Geometric measure for entanglement in n-qudit pure states, Phys. Rev. A **80**, 042302 (2009).

[30] G. Vidal, Entanglement monotones, Journal of Modern Optics **47**, 355–376 (2000).

[31] Y. Guo, Strict entanglement monotonicity under local operations and classical communication, Phys. Rev. A **99**, 022338 (2019).

[32] G. Gibbons, Typical states and density matrices, Journal of Geometry and Physics **8**, 147 (1992).

[33] V. Vedral and M. B. Plenio, Entanglement measures and purification procedures, Phys. Rev. A **57**, 1619 (1998).

[34] M. B. Plenio, Logarithmic negativity: A full entanglement monotone that is not convex, Phys. Rev. Lett. **95**, 090503 (2005).

[35] S. Hill and W. K. Wootters, Entanglement of a pair of quantum bits, Phys. Rev. Lett. **78**, 5022 (1997).

[36] A. Uhlmann, Fidelity and concurrence of conjugated states, Phys. Rev. A **62**, 032307 (2000).

[37] D. M. Greenberger, M. A. Horne, and A. Zeilinger, Going beyond bell's theorem, in *Bell's Theorem, Quantum Theory and Conceptions of the Universe*, edited by M. Kafatos (Springer Netherlands, Dordrecht, 1989) pp. 69–72.